Lecture 3.1: Integer Chern Insulators & Competing States in $tMoTe_2$

吴冯成
武汉大学

Integer Topological States

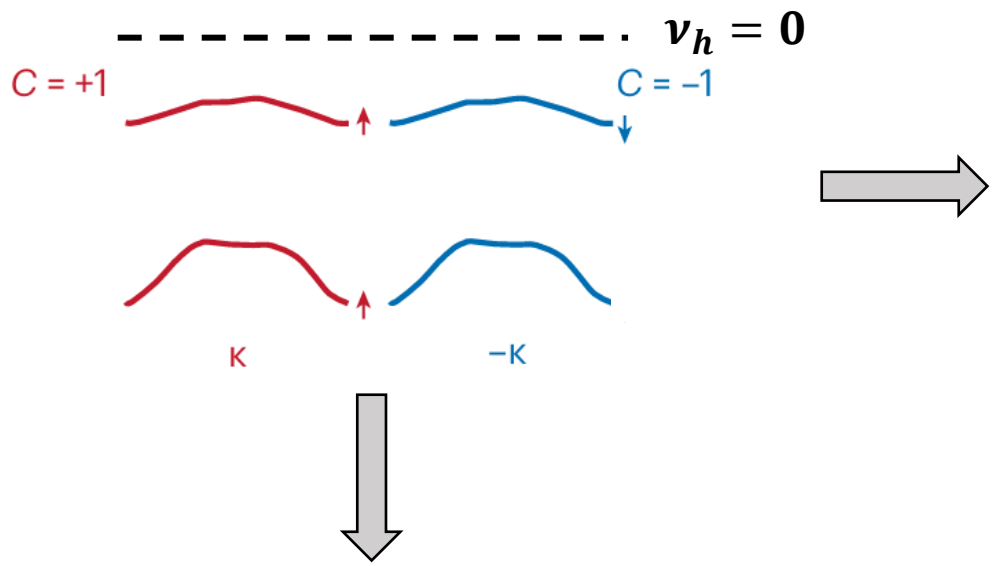

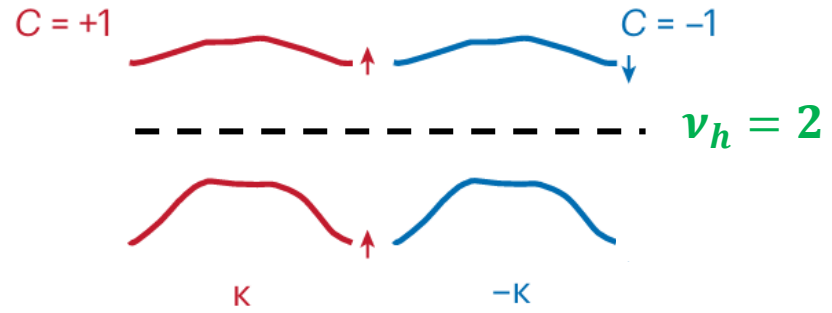

Quantum Spin Hall Insulator

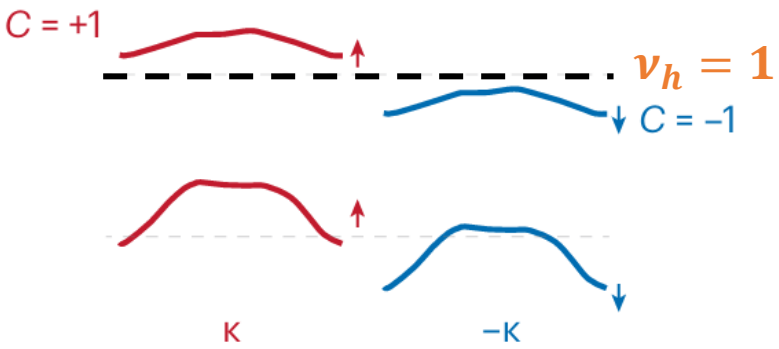

Quantum Anomalous Hall Insulator

Other Competing States?

Outline

- ✓ Kane-Mele-Hubbard Model
- ✓ Full Model

Kane-Mele-Hubbard Model

- Kane-Mele-Hubbard model:

$$H = H_{\mathrm{KM}} + U \sum_{i,\alpha} \hat{n}_{i\alpha\uparrow}\hat{n}_{i\alpha\downarrow} + \frac{V_z}{2} \sum_{i,\alpha} \ell_\alpha \hat{n}_{i\alpha}$$

$$H_{\mathrm{KM}} = t_1 \sum_{\langle ij\rangle,\alpha\neq\beta,s} c^\dagger_{i\alpha s} c_{j\beta s} + |t_2| \sum_{\langle\langle ij\rangle\rangle,\alpha,s} e^{i\phi s \epsilon_{ij}} c^\dagger_{i\alpha s} c_{j\alpha s} + \cdots$$

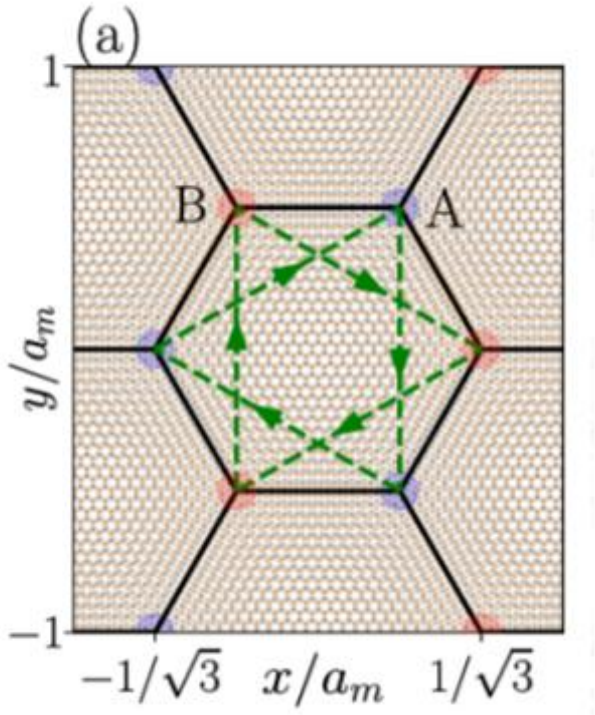

Kane-Mele-Hubbard Model

- Kane-Mele-Hubbard model:

$$H = H_{\mathrm{KM}} + U \sum_{i,\alpha} \hat{n}_{i\alpha\uparrow}\hat{n}_{i\alpha\downarrow} + \frac{V_z}{2} \sum_{i,\alpha} \ell_\alpha \hat{n}_{i\alpha}$$

$$H_{\mathrm{KM}} = t_1 \sum_{\langle ij\rangle,\alpha\neq\beta,s} c^\dagger_{i\alpha s} c_{j\beta s} + |t_2| \sum_{\langle\langle ij\rangle\rangle,\alpha,s} e^{i\phi s \epsilon_{ij}} c^\dagger_{i\alpha s} c_{j\alpha s} + \cdots$$

- Hartree-Fock Approximation:

$$n_\uparrow n_\downarrow \approx \frac{-n_0^2 + m^2}{4} + \frac{1}{2} n_0 (n_\uparrow + n_\downarrow) - \frac{1}{2} c^\dagger (\boldsymbol{m}\cdot\boldsymbol{s}) c$$

$$n_0 = \langle n_\uparrow + n_\downarrow \rangle \qquad \boldsymbol{m} = \langle c^\dagger \boldsymbol{s} c \rangle$$

$\langle \ldots \rangle$ represents the mean-field average value

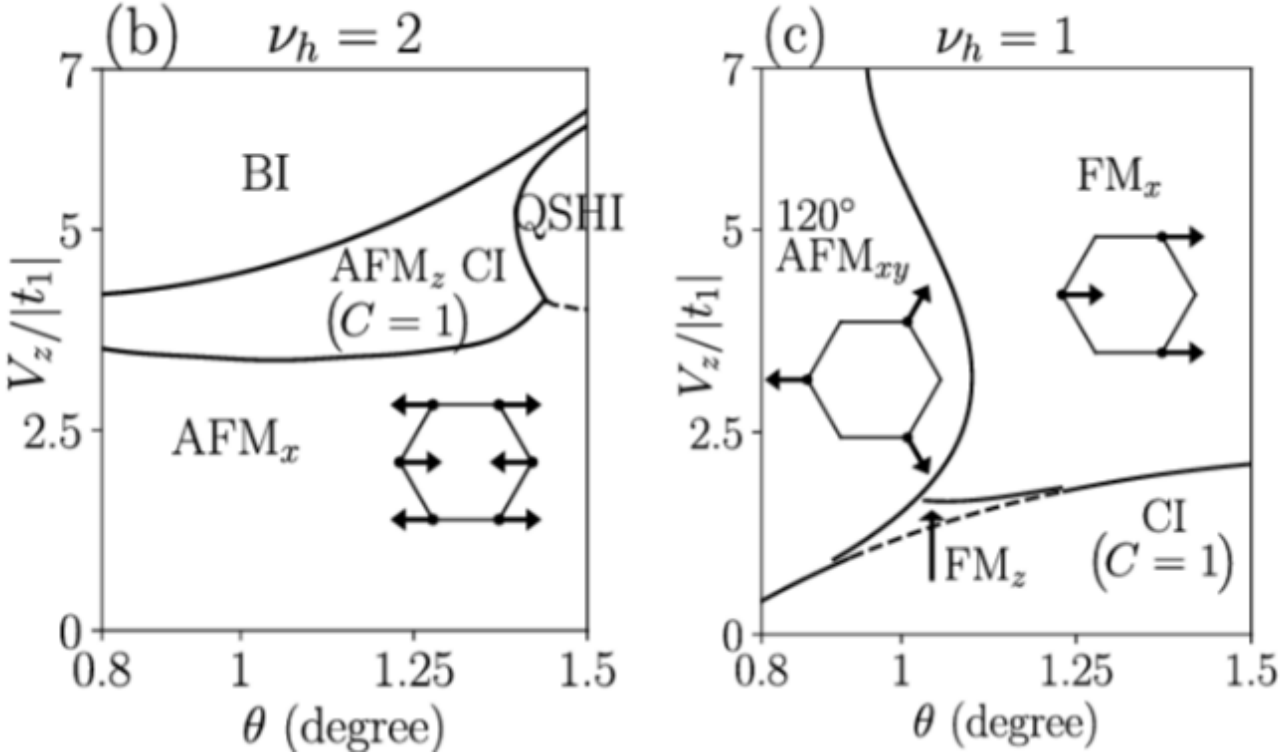

Outline

- ✓ Kane-Mele-Hubbard Model
- ✓ Full Model

Construction of Three-Orbital Model

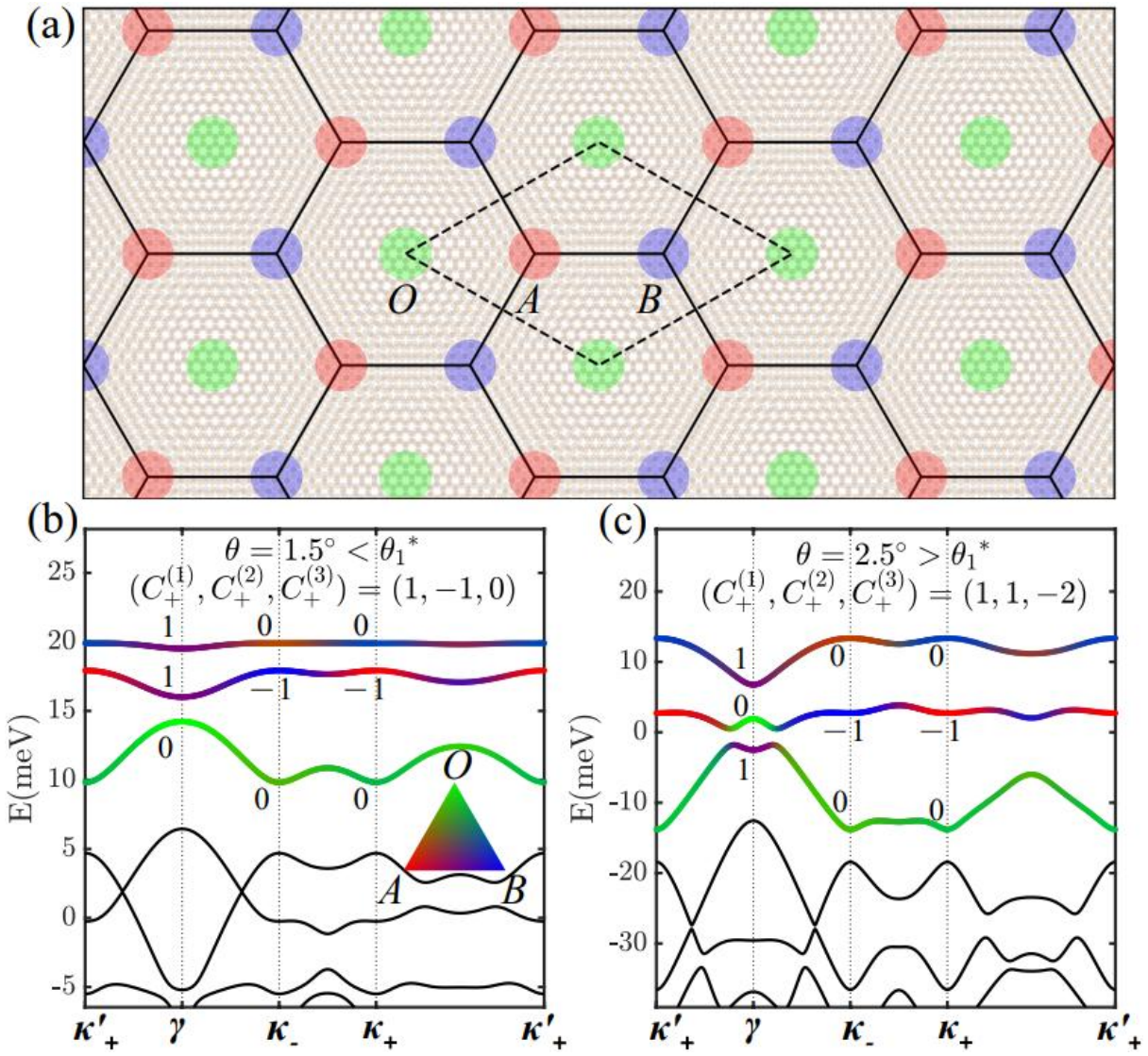

- Wannier states:

$$W^{n\tau}(\boldsymbol{r}) = \frac{1}{\sqrt{N}} \sum_{\boldsymbol{k}} \phi_{\boldsymbol{k}}^{n\tau}(\boldsymbol{r})$$

$$\phi_{\boldsymbol{k}}^{n\tau}(\boldsymbol{r}) = \sum_{n'=1,2,3} U_{\boldsymbol{k}\tau}^{n'n} \psi_{\boldsymbol{k}}^{n'\tau}(\boldsymbol{r})$$

- Disentangling by layer polarization σ_z:

$$\Pi_{\boldsymbol{k}\tau} = \begin{pmatrix} \langle \psi_{\boldsymbol{k}}^{1\tau} | \sigma_z | \psi_{\boldsymbol{k}}^{1\tau} \rangle & \langle \psi_{\boldsymbol{k}}^{1\tau} | \sigma_z | \psi_{\boldsymbol{k}}^{2\tau} \rangle & \langle \psi_{\boldsymbol{k}}^{1\tau} | \sigma_z | \psi_{\boldsymbol{k}}^{3\tau} \rangle \\ \langle \psi_{\boldsymbol{k}}^{2\tau} | \sigma_z | \psi_{\boldsymbol{k}}^{1\tau} \rangle & \langle \psi_{\boldsymbol{k}}^{2\tau} | \sigma_z | \psi_{\boldsymbol{k}}^{2\tau} \rangle & \langle \psi_{\boldsymbol{k}}^{2\tau} | \sigma_z | \psi_{\boldsymbol{k}}^{3\tau} \rangle \\ \langle \psi_{\boldsymbol{k}}^{3\tau} | \sigma_z | \psi_{\boldsymbol{k}}^{1\tau} \rangle & \langle \psi_{\boldsymbol{k}}^{3\tau} | \sigma_z | \psi_{\boldsymbol{k}}^{2\tau} \rangle & \langle \psi_{\boldsymbol{k}}^{3\tau} | \sigma_z | \psi_{\boldsymbol{k}}^{3\tau} \rangle \end{pmatrix}$$

$$U_{\boldsymbol{k}\tau}^{\dagger} \Pi_{\boldsymbol{k}\tau} U_{\boldsymbol{k}\tau} = \begin{pmatrix} \rho_{\boldsymbol{k}}^{1\tau} & 0 & 0 \\ 0 & \rho_{\boldsymbol{k}}^{2\tau} & 0 \\ 0 & 0 & \rho_{\boldsymbol{k}}^{3\tau} \end{pmatrix}$$

Construction of Three-Orbital Model

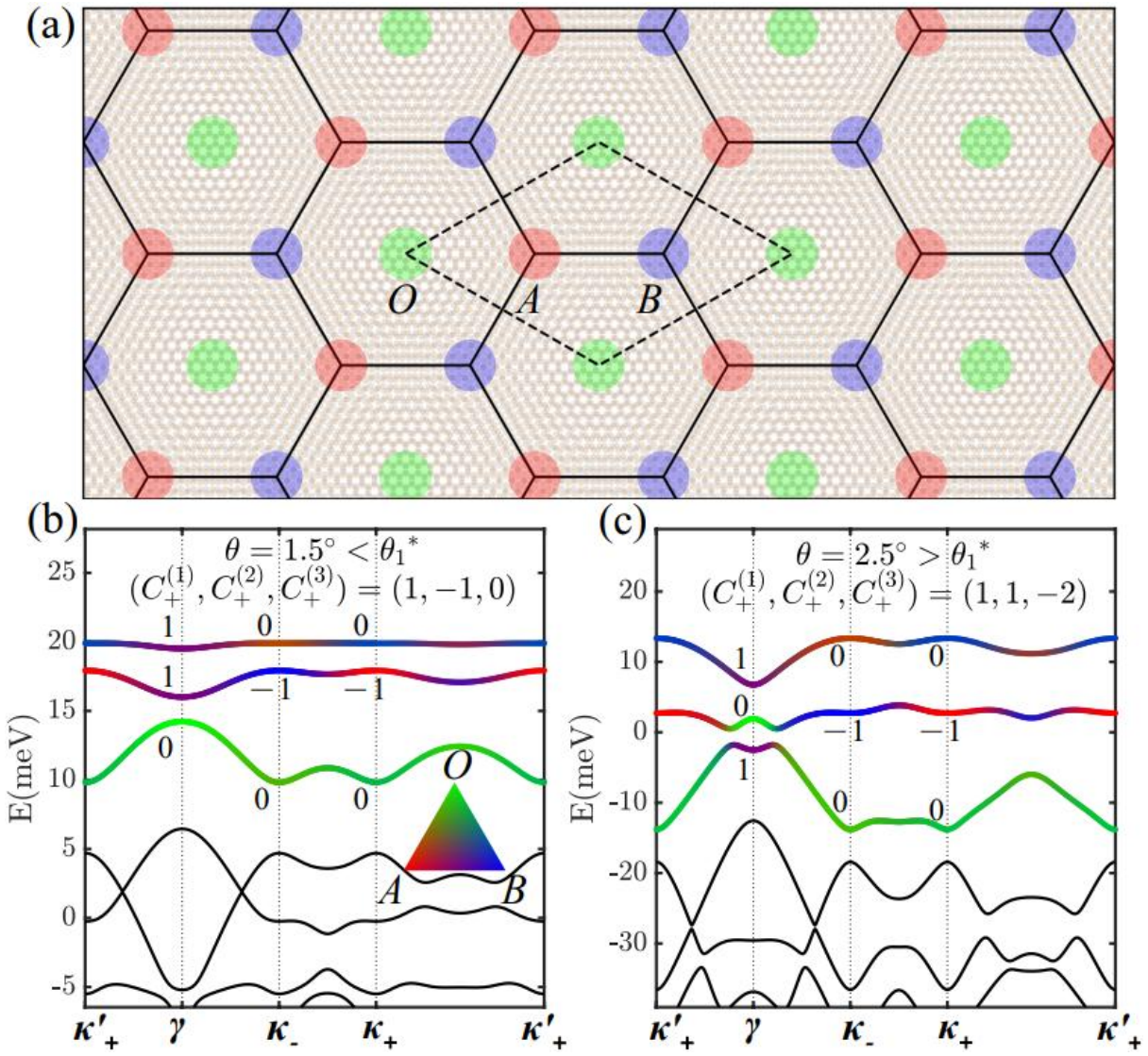

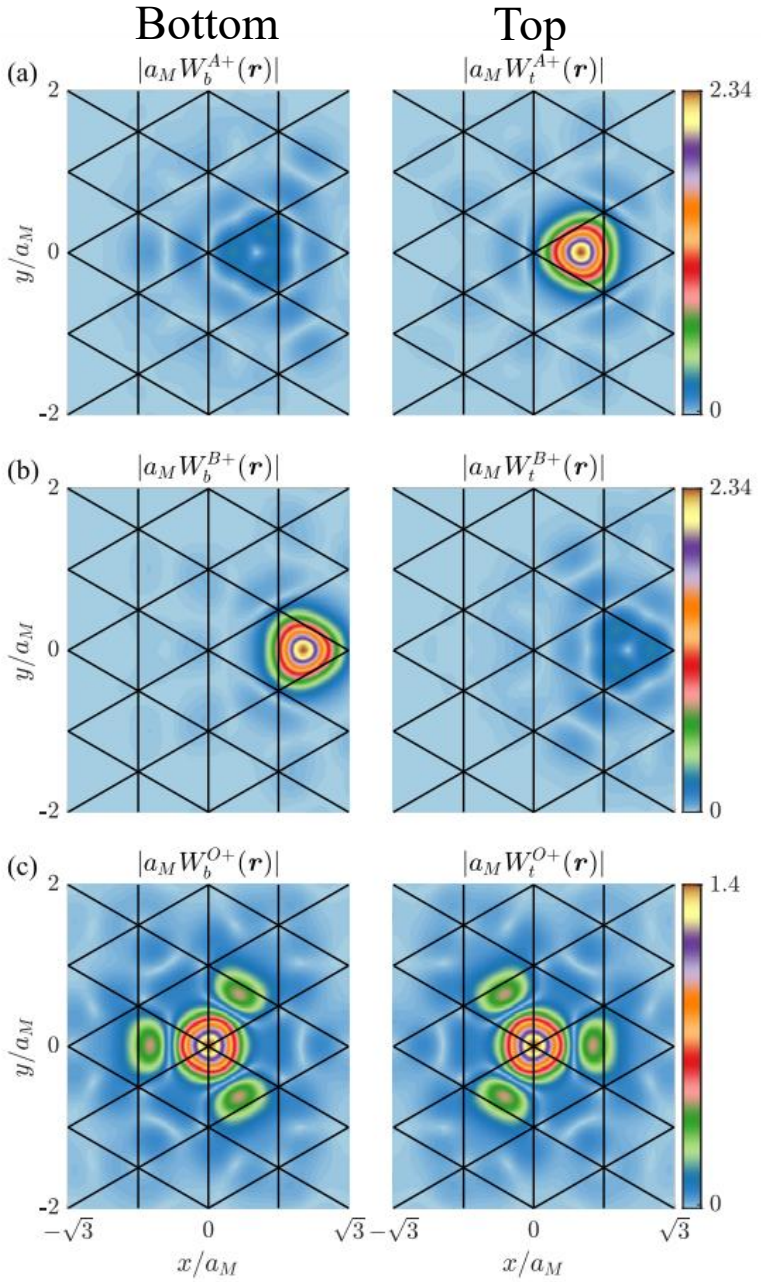

A orbital

B orbital

O orbital

Single-Particle Model

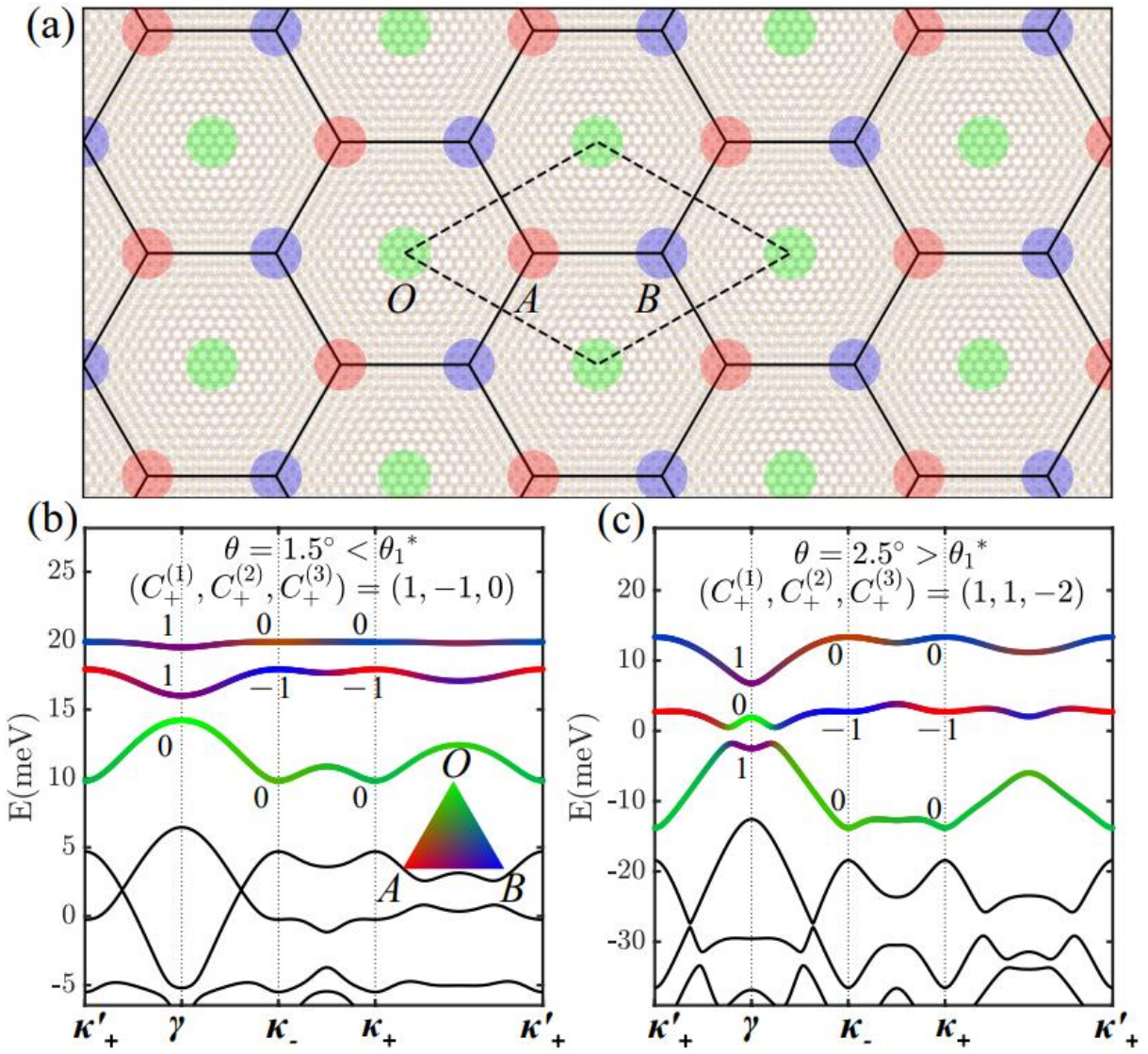

Single-particle Hamiltonian in the Wannier basis:

$$\hat{\mathcal{H}}_0 = \sum_{\boldsymbol{k},\tau,n,n'} h_{\boldsymbol{k}\tau}^{nn'} c_{\boldsymbol{k}n\tau}^\dagger c_{\boldsymbol{k}n'\tau},$$

$$h_{\boldsymbol{k}\tau} = U_{\boldsymbol{k}\tau}^\dagger \begin{pmatrix} E_{\boldsymbol{k}}^{1\tau} & 0 & 0 \\ 0 & E_{\boldsymbol{k}}^{2\tau} & 0 \\ 0 & 0 & E_{\boldsymbol{k}}^{3\tau} \end{pmatrix} U_{\boldsymbol{k}\tau}.$$

Interacting Model

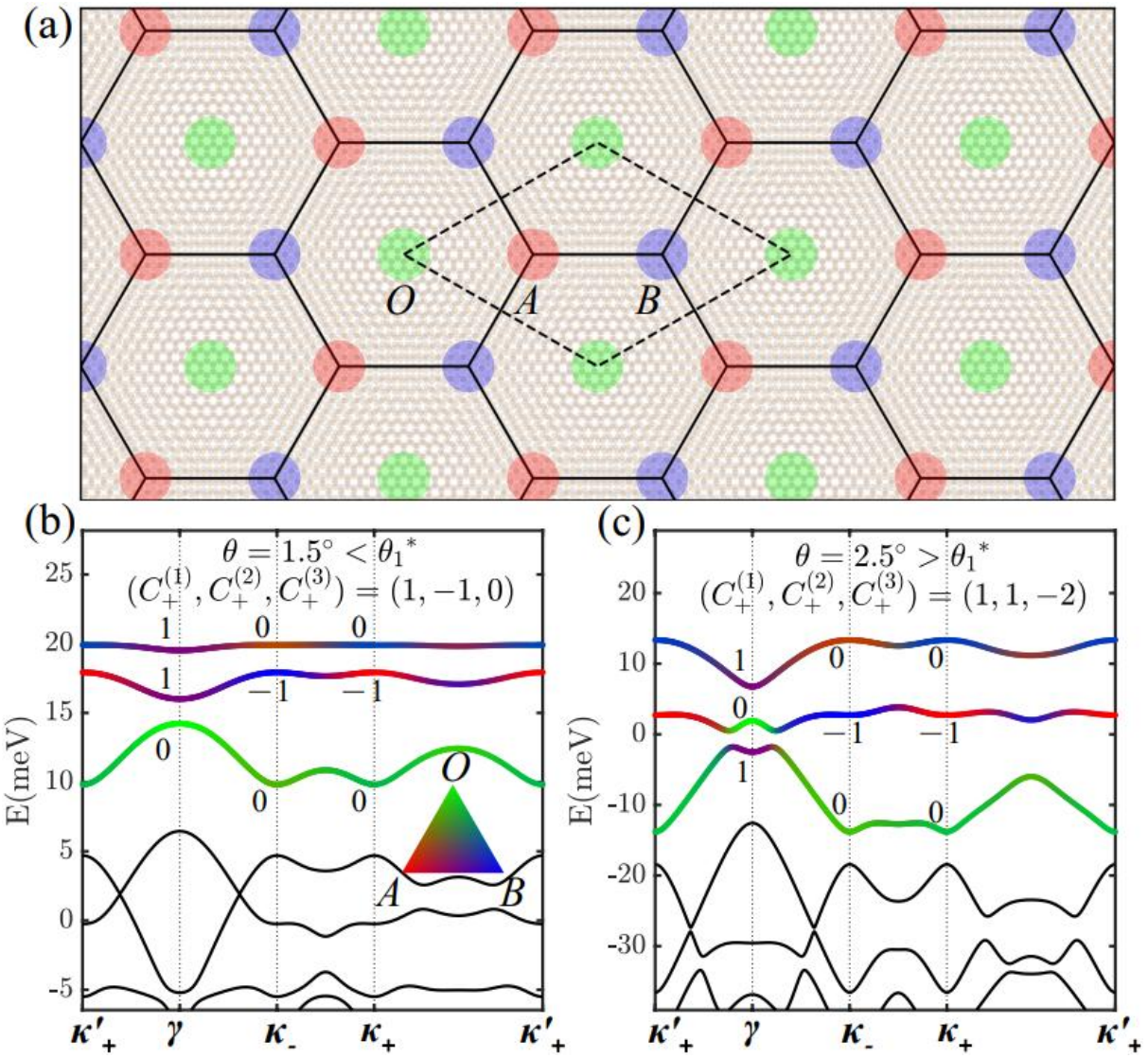

Particle-hole transformation:

$$\hat{\mathcal{H}}_0 = -\sum_{\boldsymbol{k},\tau,n,n'} [h_{\boldsymbol{k}\tau}^{\top}]^{nn'} b_{\boldsymbol{k}n\tau}^{\dagger} b_{\boldsymbol{k}n'\tau},$$

Coulomb matrix element constructed **directly in k-space**:

$$\hat{\mathcal{H}}_{\text{int}} = \frac{1}{2}\sum V_{\boldsymbol{k}_1\boldsymbol{k}_2\boldsymbol{k}_3\boldsymbol{k}_4}^{n_1n_2n_3n_4}(\tau,\tau')\, b_{\boldsymbol{k}_1n_1\tau}^{+} b_{\boldsymbol{k}_2n_2\tau'}^{+} b_{\boldsymbol{k}_3n_3\tau'} b_{\boldsymbol{k}_4n_4\tau},$$

$$V_{\boldsymbol{k}_1\boldsymbol{k}_2\boldsymbol{k}_3\boldsymbol{k}_4}^{n_1n_2n_3n_4}(\tau,\tau') = \frac{1}{\mathcal{A}}\sum_{\boldsymbol{q}} V_{\boldsymbol{q}} M_{\boldsymbol{k}_1\boldsymbol{k}_4}^{n_1n_4}(\tau,\boldsymbol{q})\, M_{\boldsymbol{k}_2\boldsymbol{k}_3}^{n_2n_3}(\tau',-\boldsymbol{q}),$$

$$M_{\boldsymbol{k}_1\boldsymbol{k}_4}^{n_1n_4}(\tau,\boldsymbol{q}) = \sum_{\ell}\int d\boldsymbol{r} e^{i\boldsymbol{q}\cdot\boldsymbol{r}} [\tilde{\phi}_{\boldsymbol{k}_1\ell}^{n_1\tau}(\boldsymbol{r})]^{*} \tilde{\phi}_{\boldsymbol{k}_4\ell}^{n_4\tau}(\boldsymbol{r}),$$

Coulomb dual-gate screened Coulomb interaction:

$$V_{\boldsymbol{q}} = 2\pi e^2 \tanh(|\boldsymbol{q}|d)/(\epsilon|\boldsymbol{q}|), \quad \tilde{\phi}_{\boldsymbol{k}}^{n\tau}(r) = [\phi_{\boldsymbol{k}}^{n\tau}(r)]^{*}$$

ν=1 Phase Diagram

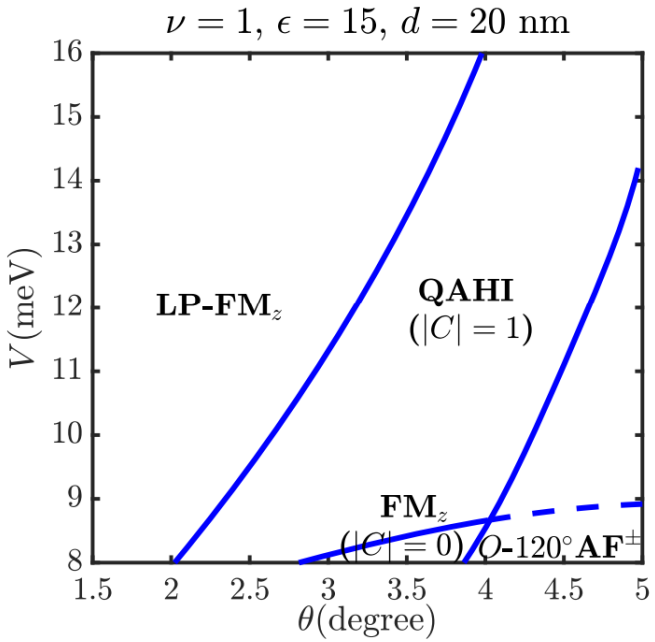

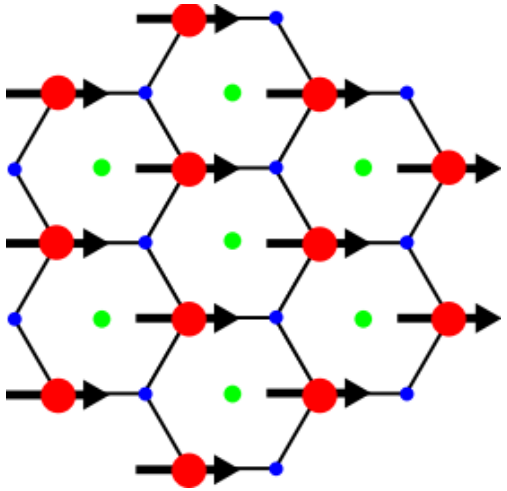

LP-FM$_x$

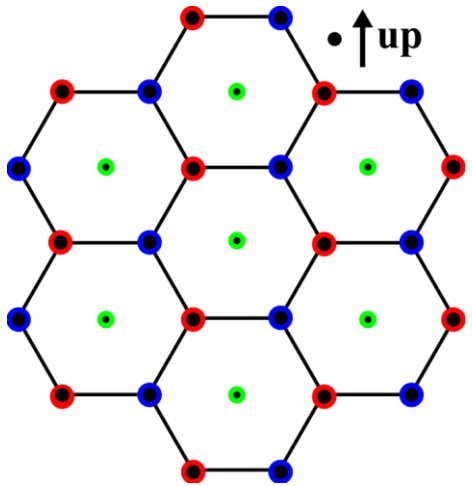

QAHI/FM$_z$

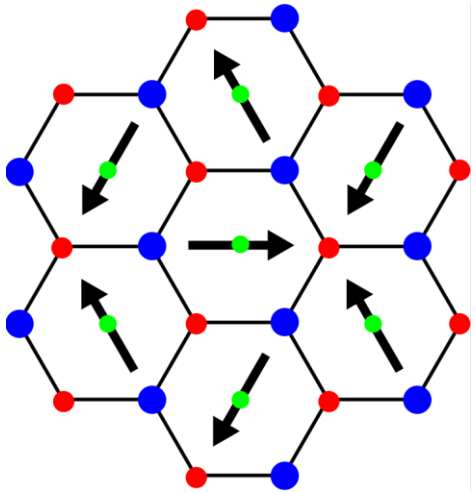

O-120° AF^{+}

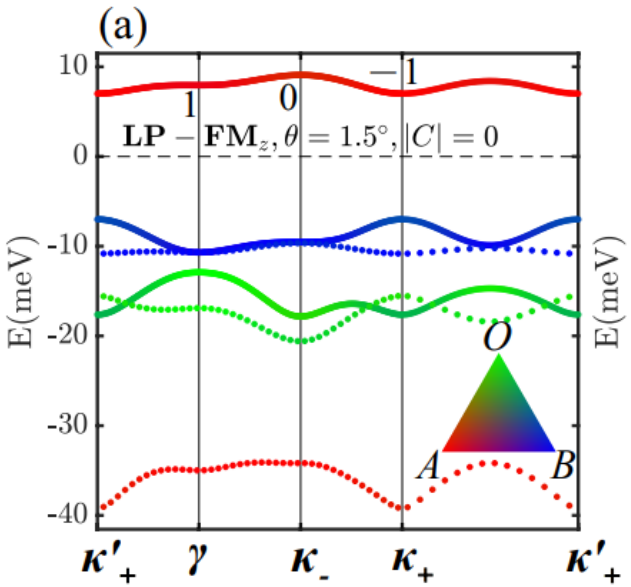

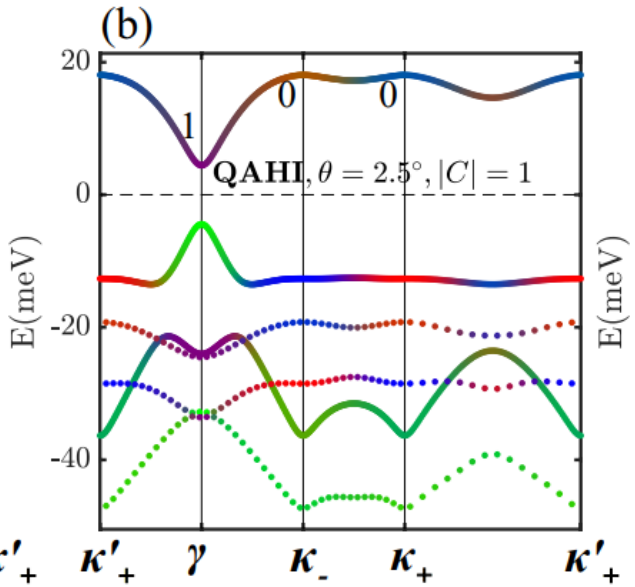

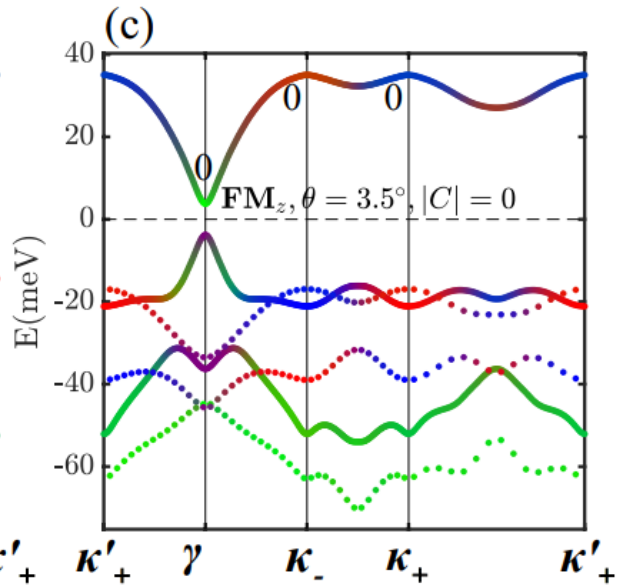

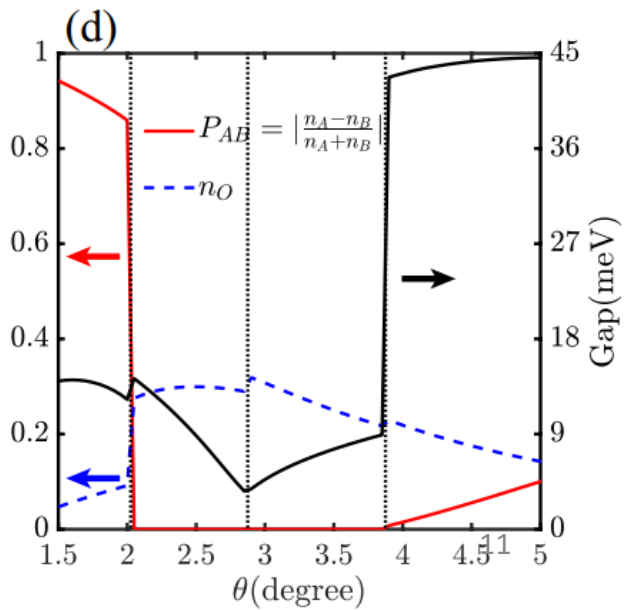

ν=1 Phase Diagram: ϵ −dependence

Phase Diagram

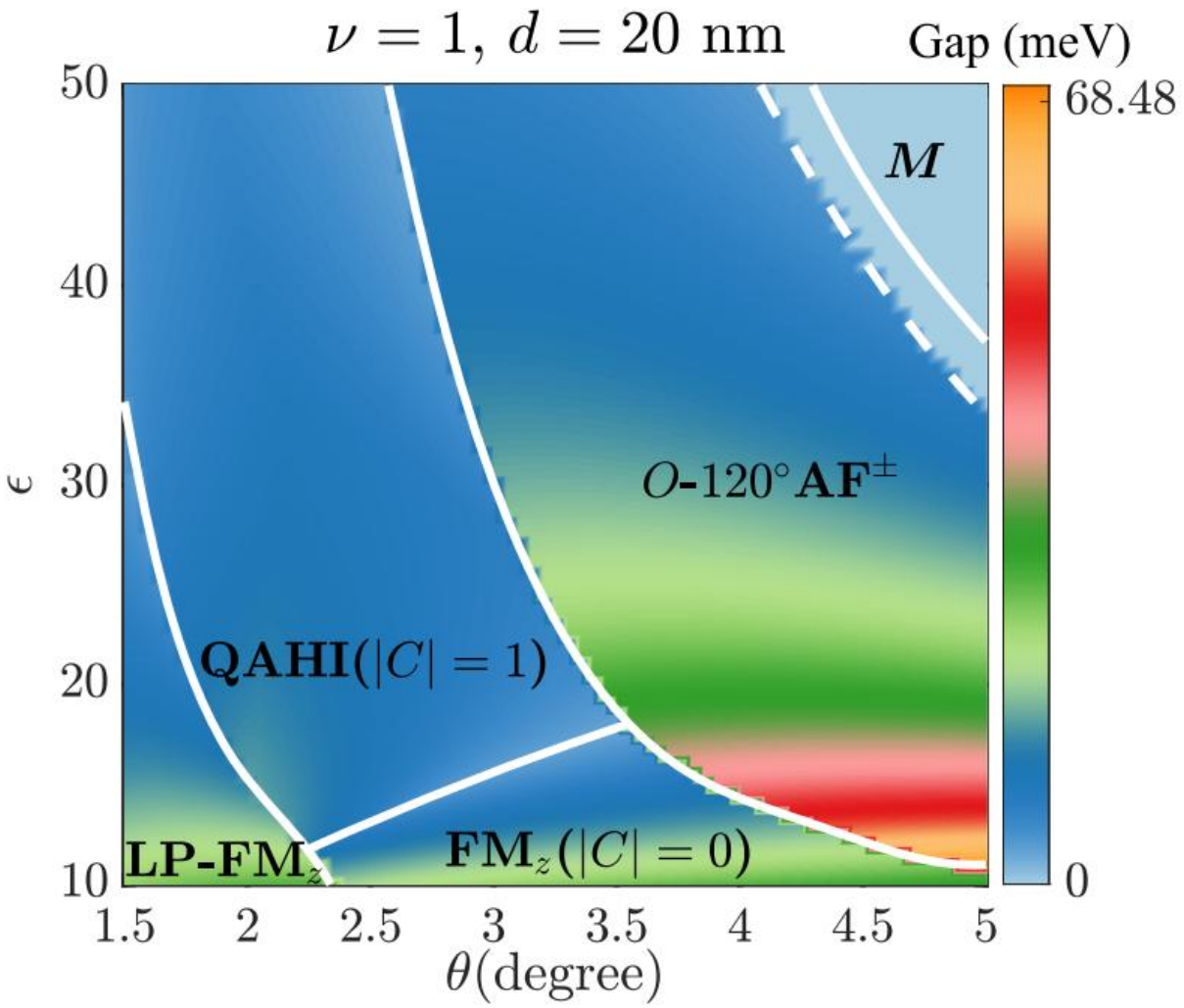

Energy Competition

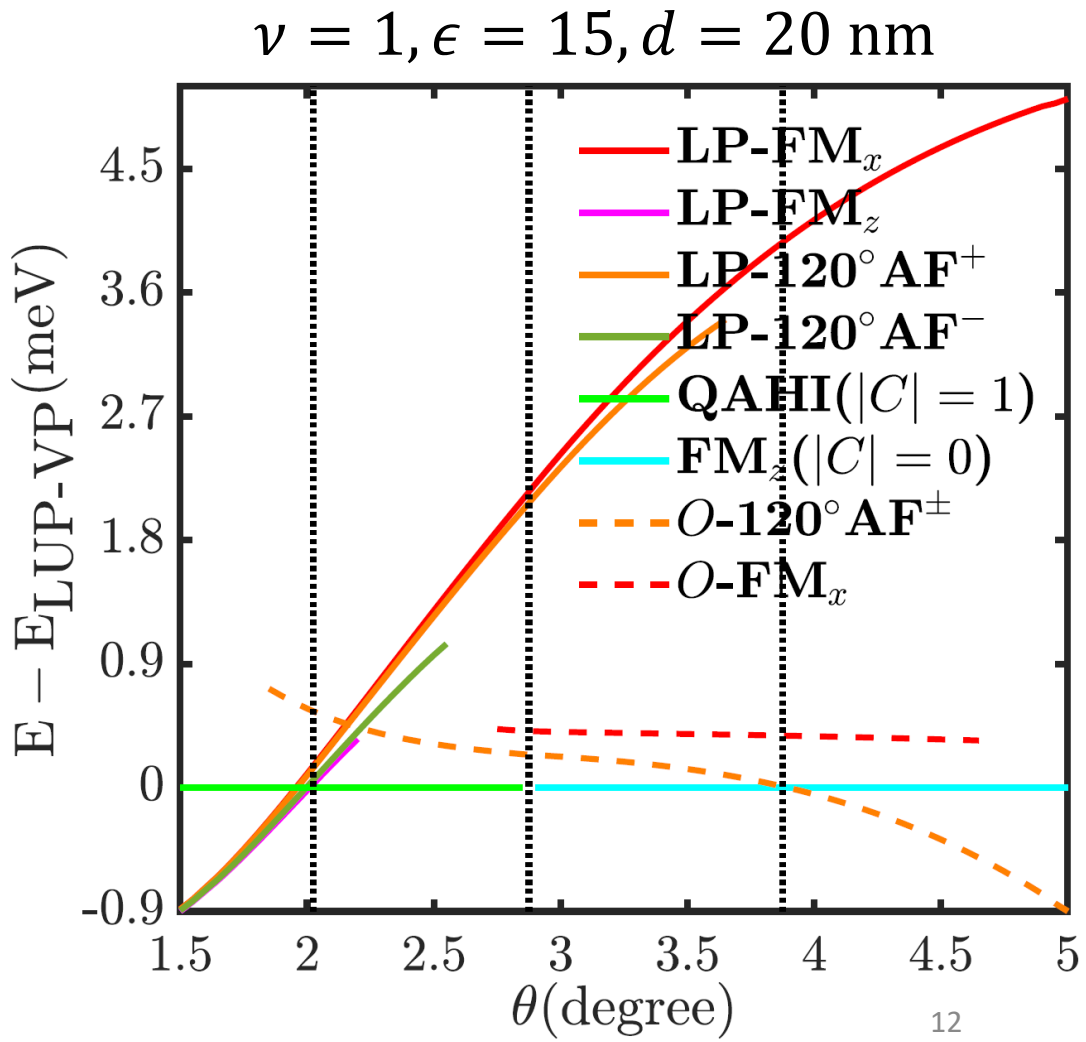

ν=2 Phase Diagram

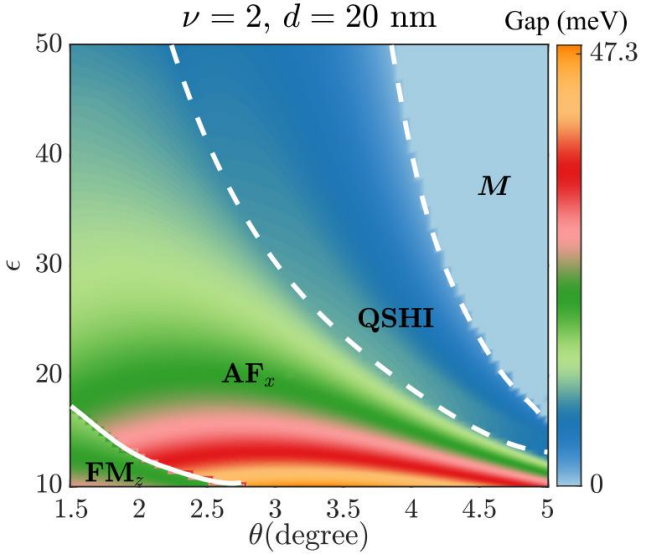

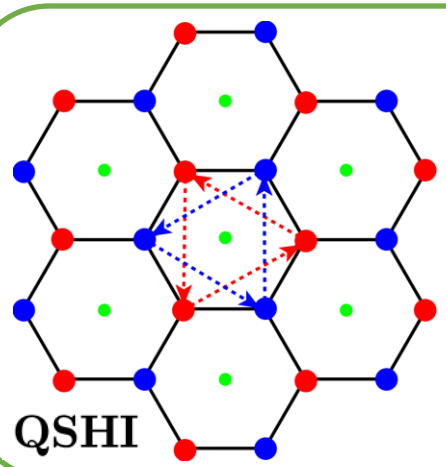

Opposite valleys with C = ±1

Valleys also act as spin

Z_2 topological invariant

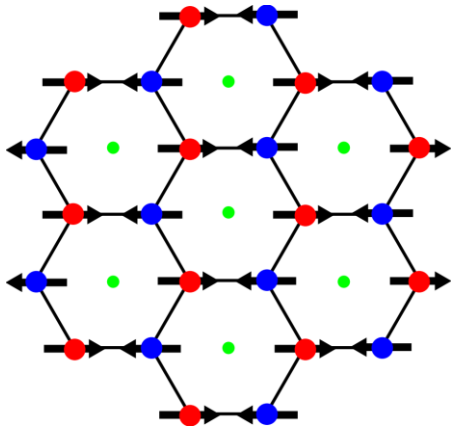

AF_x

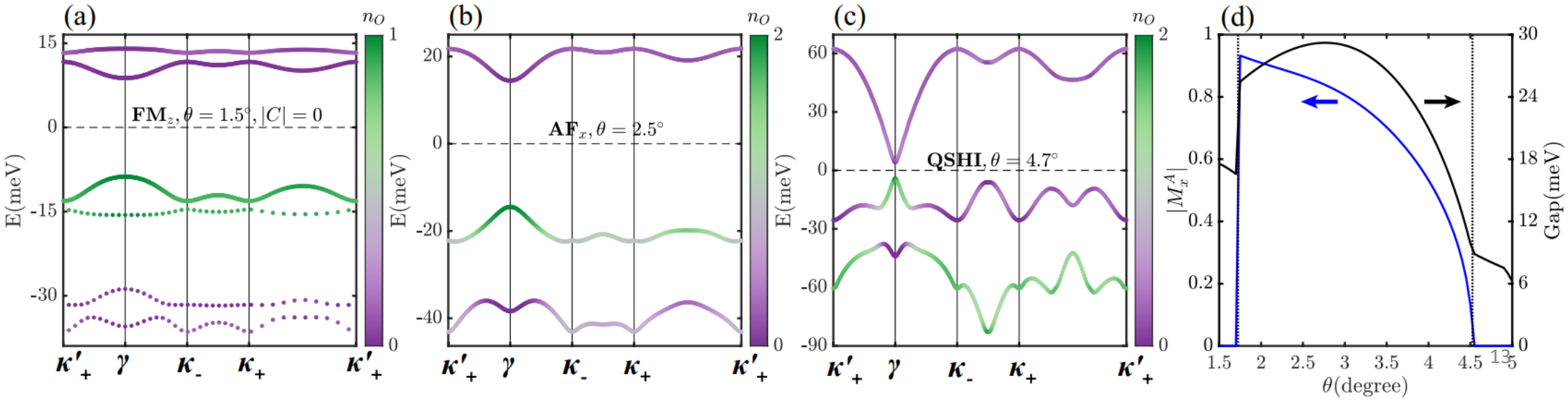

Interaction-Driven Phase Diagram at Integer Fillings

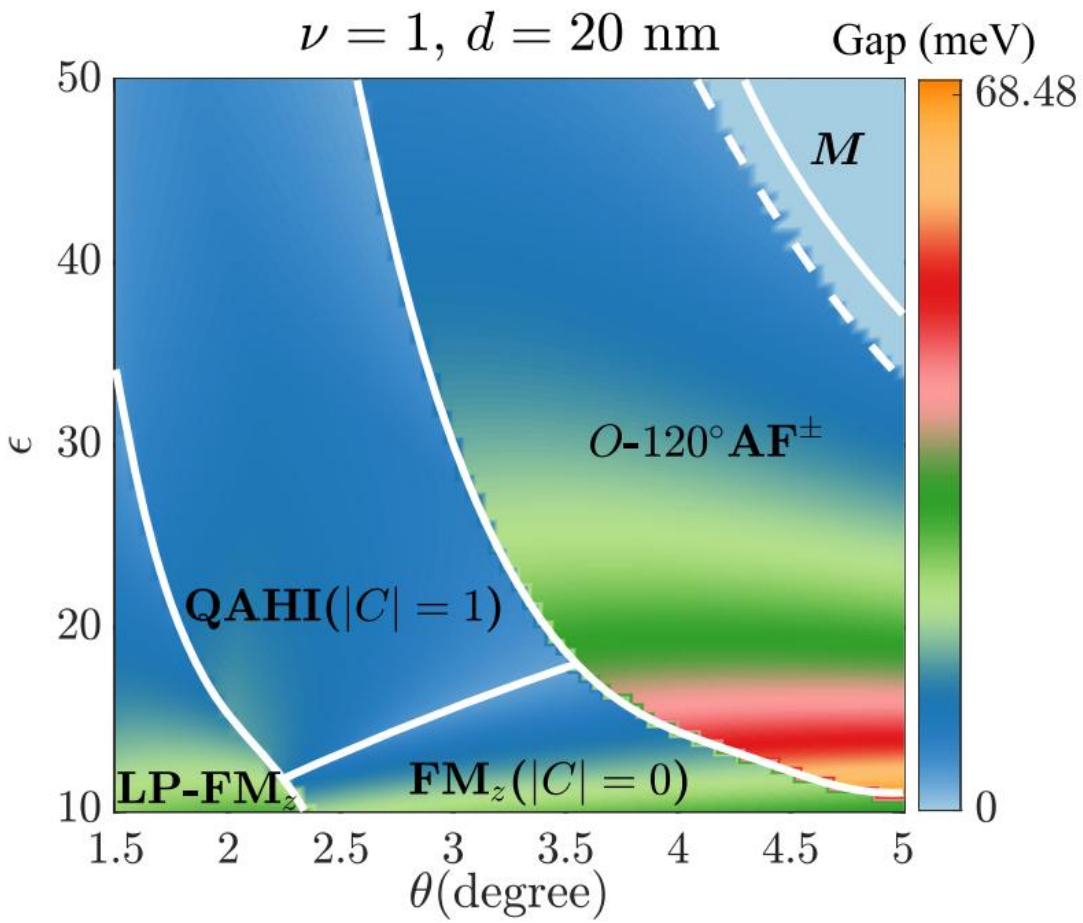

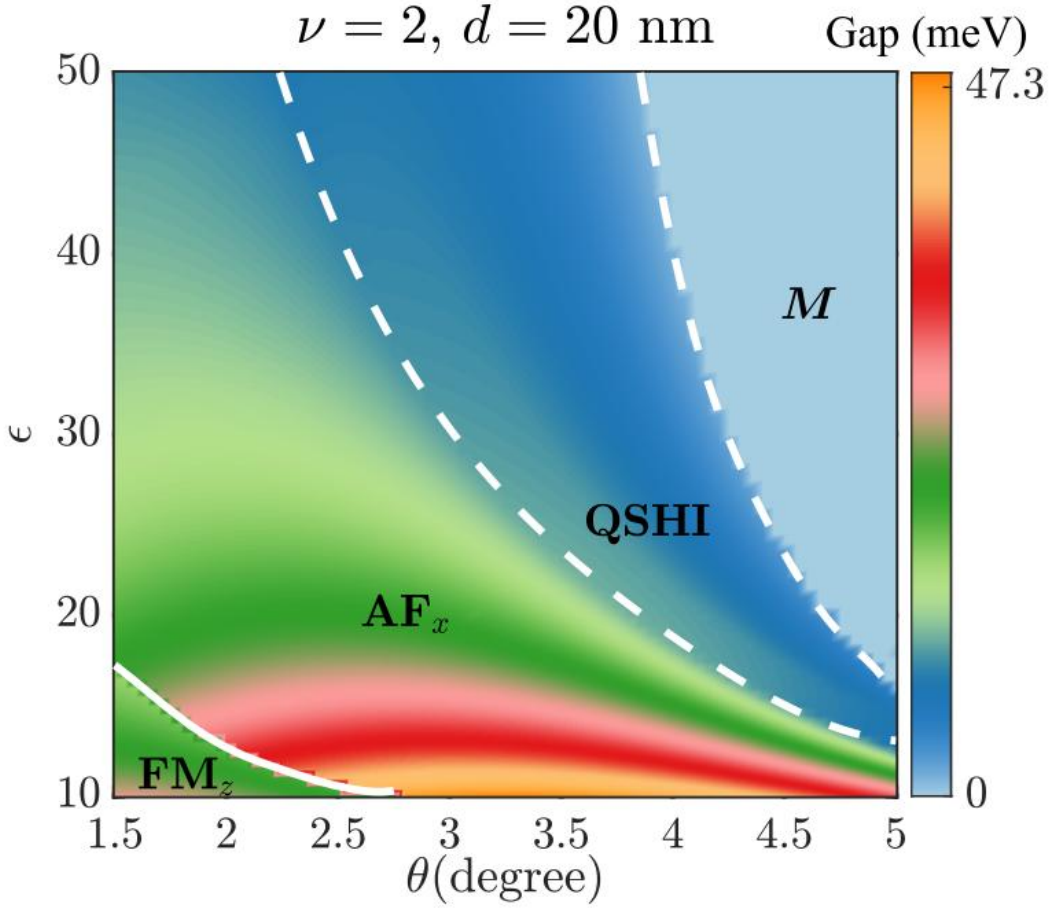

- W.-X. Qiu, B. Li, X. Luo, **FW**, PRX **13**, 041026 (2023)
- B. Li, W.-X. Qiu, **FW**, PRB **109**, L041106 (2024)

Hartree-Fock in the Plane-Wave Basis

In this section, we include the Coulomb interaction and derive the mean-field Hamiltonian by applying the Hartree-Fock (HF) approximation. We first rewrite $\hat{\mathcal{H}}_0$ in the momentum space with the creation operator being defined as $c^\dagger_{\boldsymbol{k},l,\tau} = \frac{1}{\sqrt{A}} \int \psi^\dagger_{l,\tau}(\boldsymbol{r}) e^{i\boldsymbol{k}\cdot\boldsymbol{r}} d^2\boldsymbol{r}$ (the spin index is absent because it can be inferred from the valley and layer indices due to the effective spin-valley-layer locking), where A is the total area. Thus, $\hat{\mathcal{H}}_0$ can be expressed as

$$\hat{\mathcal{H}}_0 = \sum_{\boldsymbol{k}_\alpha,\boldsymbol{k}_\beta} \sum_{l_\alpha,l_\beta} \sum_{\tau} h^{(\tau)}_{\boldsymbol{k}_\alpha l_\alpha,\boldsymbol{k}_\beta l_\beta} c^\dagger_{\boldsymbol{k}_\alpha,l_\alpha,\tau} c_{\boldsymbol{k}_\beta,l_\beta,\tau}, \tag{S6}$$

where $h^{(\tau)}$ is the Hamiltonian H_τ expanded in the plane-wave basis, and the momentum $\boldsymbol{k}$ is defined in the extended Brillouin zone that spans the full momentum space, i.e., $\boldsymbol{k} \in \mathbb{R}^2$. Here, the subscripts α, β are index for momenta. Due to Bloch's theorem, $h^{(\tau)}_{\boldsymbol{k}_\alpha l_\alpha,\boldsymbol{k}_\beta l_\beta}$ is nonzero only when $\boldsymbol{k}_\alpha - \boldsymbol{k}_\beta$ is equal to the linear combination of any multiples of hone of the moiré reciprocal lattice vectors (including the zero vector).

At the charge neutrality (filling factor $\nu = 0$) of the heterobilayer, all valence bands are below Fermi energy. We are interested in situations where the valence bands are slightly hole-doped. Therefore, it is convenient to study the many-body interaction in the hole basis. We define the hole operator as $b_{\boldsymbol{k},l,\tau} = c^\dagger_{\boldsymbol{k},l,\tau}$, and $\hat{\mathcal{H}}_0$ in the hole basis is

$$\hat{\mathcal{H}}_0 = \sum_{\tau} \operatorname{Tr} h^{(\tau)} - \sum_{\boldsymbol{k}_\alpha,\boldsymbol{k}_\beta} \sum_{l_\alpha,l_\beta} \sum_{\tau} [h^{(\tau)}]^{\intercal}_{\boldsymbol{k}_\alpha l_\alpha,\boldsymbol{k}_\beta l_\beta} b^\dagger_{\boldsymbol{k}_\alpha,l_\alpha,\tau} b_{\boldsymbol{k}_\beta,l_\beta,\tau} \tag{S7}$$

Hartree-Fock in the Plane-Wave Basis

By combing the single-particle Hamiltonian with the hole-hole Coulomb interaction term, we obtain the full Hamiltonian (dropping the constant term) as

$$\begin{aligned}
\hat{\mathcal{H}} &= \hat{\mathcal{H}}_1 + \hat{\mathcal{H}}_{\text{int}}, \\
\hat{\mathcal{H}}_1 &= \sum_{\boldsymbol{k}_\alpha,\boldsymbol{k}_\beta} \sum_{l_\alpha,l_\beta} \sum_{\tau} \tilde{h}^{(\tau)}_{\boldsymbol{k}_\alpha l_\alpha,\boldsymbol{k}_\beta l_\beta} b^\dagger_{\boldsymbol{k}_\alpha,l_\alpha,\tau} b_{\boldsymbol{k}_\beta,l_\beta,\tau}, \\
\hat{\mathcal{H}}_{\text{int}} &= \frac{1}{2A} \sum_{\boldsymbol{k}_\alpha,\boldsymbol{k}_\beta,\boldsymbol{k}_\gamma,\boldsymbol{k}_\delta} \sum_{l_\alpha,l_\beta} \sum_{\tau_\alpha,\tau_\beta} V(\boldsymbol{k}_\alpha - \boldsymbol{k}_\delta) b^\dagger_{\boldsymbol{k}_\alpha,l_\alpha,\tau_\alpha} b^\dagger_{\boldsymbol{k}_\beta,l_\beta,\tau_\beta} b_{\boldsymbol{k}_\gamma,l_\beta,\tau_\beta} b_{\boldsymbol{k}_\delta,l_\alpha,\tau_\alpha} \delta_{\boldsymbol{k}_\alpha+\boldsymbol{k}_\beta,\boldsymbol{k}_\delta+\boldsymbol{k}_\gamma},
\end{aligned} \tag{S8}$$

where $\tilde{h}^{(\tau)} = -[h^{(\tau)}]^\intercal$, the dual-gate screened Coulomb interaction $V(\boldsymbol{k}) = 2\pi e^2 \tanh(|\boldsymbol{k}|d)/(\epsilon|\boldsymbol{k}|)$, d is the sample-to-gate distance, and ϵ is the dielectric constant.

Using the HF approximation, we obtain the following mean-field Hamiltonian $\hat{H}^{\text{HF}}$,

$$\begin{aligned}
\hat{\mathcal{H}}^{\text{HF}} &= \hat{\mathcal{H}}_1 + \hat{\mathcal{H}}^{\text{HF}}_{\text{int}}, \\
\hat{\mathcal{H}}^{\text{HF}}_{\text{int}} &= \frac{1}{A} \sum_{\boldsymbol{k}_\alpha,\boldsymbol{k}_\beta,\boldsymbol{k}_\gamma,\boldsymbol{k}_\delta} \sum_{l_\alpha,l_\beta} \sum_{\tau_\alpha,\tau_\beta} V(\boldsymbol{k}_\alpha - \boldsymbol{k}_\delta) \Big(\Big\langle b^\dagger_{\boldsymbol{k}_\alpha,l_\alpha,\tau_\alpha} b_{\boldsymbol{k}_\delta,l_\alpha,\tau_\alpha} \Big\rangle b^\dagger_{\boldsymbol{k}_\beta,l_\beta,\tau_\beta} b_{\boldsymbol{k}_\gamma,l_\beta,\tau_\beta} \\
&\quad - \Big\langle b^\dagger_{\boldsymbol{k}_\alpha,l_\alpha,\tau_\alpha} b_{\boldsymbol{k}_\gamma,l_\beta,\tau_\beta} \Big\rangle b^\dagger_{\boldsymbol{k}_\beta,l_\beta,\tau_\beta} b_{\boldsymbol{k}_\delta,l_\alpha,\tau_\alpha} \Big) \delta_{\boldsymbol{k}_\alpha+\boldsymbol{k}_\beta,\boldsymbol{k}_\delta+\boldsymbol{k}_\gamma}.
\end{aligned} \tag{S9}$$

Hartree-Fock in the Plane-Wave Basis

The Hartree-Fock solution can either preserve or spontaneously break the moiré lattice translational symmetry. In our study, we always assume that the interaction-induced states have a real-space unit cell that is commensurate with the moiré unit cell, but the former can be larger than the latter, for example in charge/spin density wave states. In $\hat{\mathcal{H}}_{\text{int}}^{\text{HF}}$, the average value $\left\langle b^{\dagger}_{\boldsymbol{k}_\alpha,l_\alpha,\tau_\alpha} b_{\boldsymbol{k}_\beta,l_\beta,\tau_\beta} \right\rangle$ is nonzero only when $\boldsymbol{k}_\alpha - \boldsymbol{k}_\beta = \boldsymbol{G}$, where $\boldsymbol{G}$ is a reciprocal lattice vector (including the zero vector) of the resulting real-space unit cell.

The total energy per moiré unit cell is obtained by averaging $\hat{H}$ in Eq. (S8), i.e.,

$$
\begin{aligned}
\left\langle \hat{\mathcal{H}} \right\rangle &= \left\langle \hat{\mathcal{H}}_1 \right\rangle + \left\langle \hat{\mathcal{H}}_{\text{int}} \right\rangle , \\
\left\langle \hat{\mathcal{H}}_1 \right\rangle &= \sum_{\boldsymbol{k}_\alpha,\boldsymbol{k}_\beta} \sum_{l_\alpha,l_\beta} \sum_{\tau} \tilde{h}^{(\tau)}_{\boldsymbol{k}_\alpha l_\alpha,\boldsymbol{k}_\beta l_\beta} \left\langle b^{\dagger}_{\boldsymbol{k}_\alpha,l_\alpha,\tau} b_{\boldsymbol{k}_\beta,l_\beta,\tau} \right\rangle , \\
\left\langle \hat{\mathcal{H}}_{\text{int}} \right\rangle &= \frac{1}{2A} \sum_{\boldsymbol{k}_\alpha,\boldsymbol{k}_\beta,\boldsymbol{k}_\gamma,\boldsymbol{k}_\delta} \sum_{l_\alpha,l_\beta} \sum_{\tau_\alpha,\tau_\beta} V(\boldsymbol{k}_\alpha - \boldsymbol{k}_\delta) \Big(\left\langle b^{\dagger}_{\boldsymbol{k}_\alpha,l_\alpha,\tau_\alpha} b_{\boldsymbol{k}_\delta,l_\alpha,\tau_\alpha} \right\rangle \left\langle b^{\dagger}_{\boldsymbol{k}_\beta,l_\beta,\tau_\beta} b_{\boldsymbol{k}_\gamma,l_\beta,\tau_\beta} \right\rangle \\
&\quad - \left\langle b^{\dagger}_{\boldsymbol{k}_\alpha,l_\alpha,\tau_\alpha} b_{\boldsymbol{k}_\gamma,l_\beta,\tau_\beta} \right\rangle \left\langle b^{\dagger}_{\boldsymbol{k}_\beta,l_\beta,\tau_\beta} b_{\boldsymbol{k}_\delta,l_\alpha,\tau_\alpha} \right\rangle \Big) \delta_{\boldsymbol{k}_\alpha+\boldsymbol{k}_\beta,\boldsymbol{k}_\delta+\boldsymbol{k}_\gamma} ,
\end{aligned}
\tag{S10}
$$

Field-tunable v=1 Phase Diagram

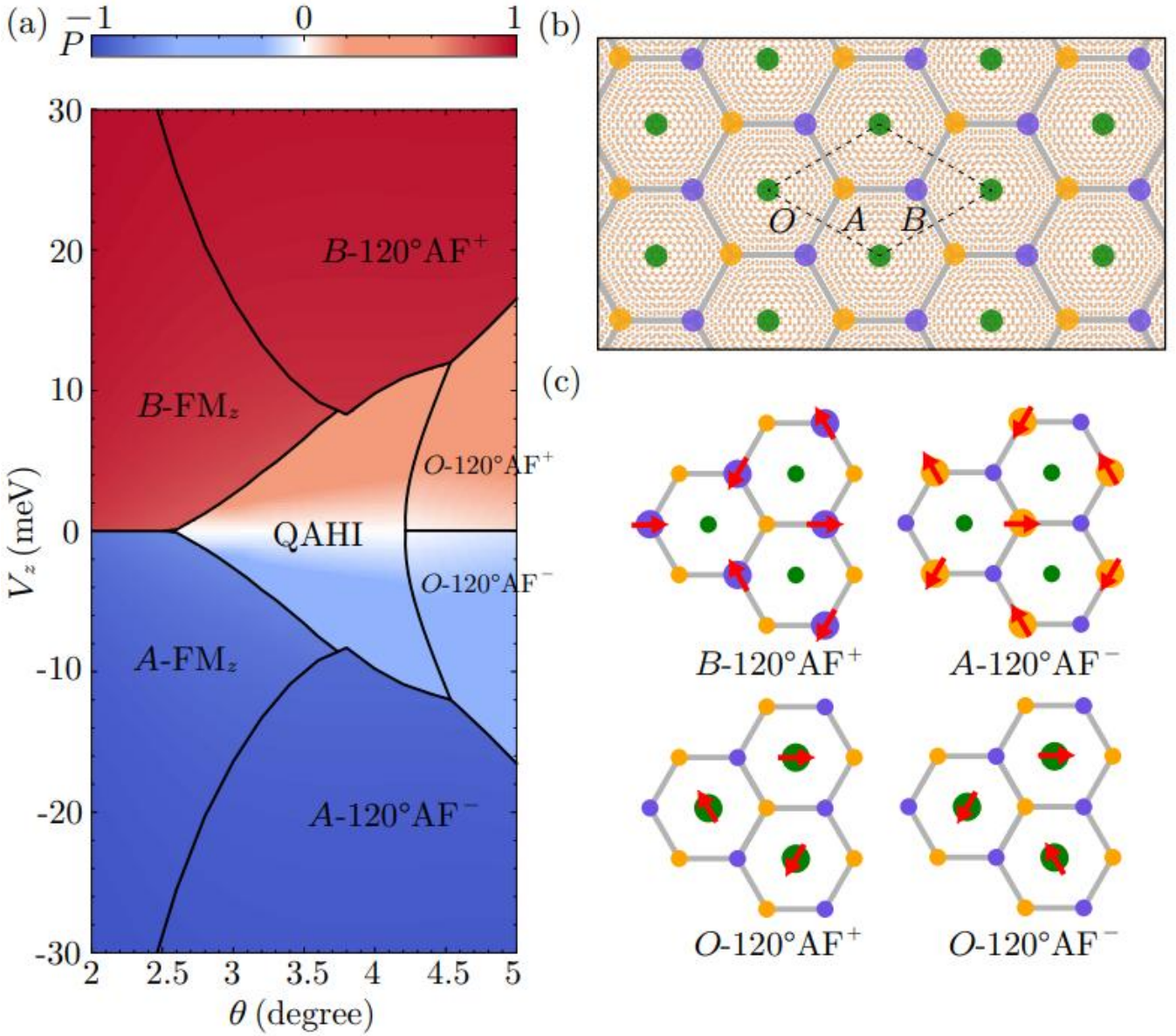

Electric-Field Tuned Phase Diagram

Theoretical Phase Diagram

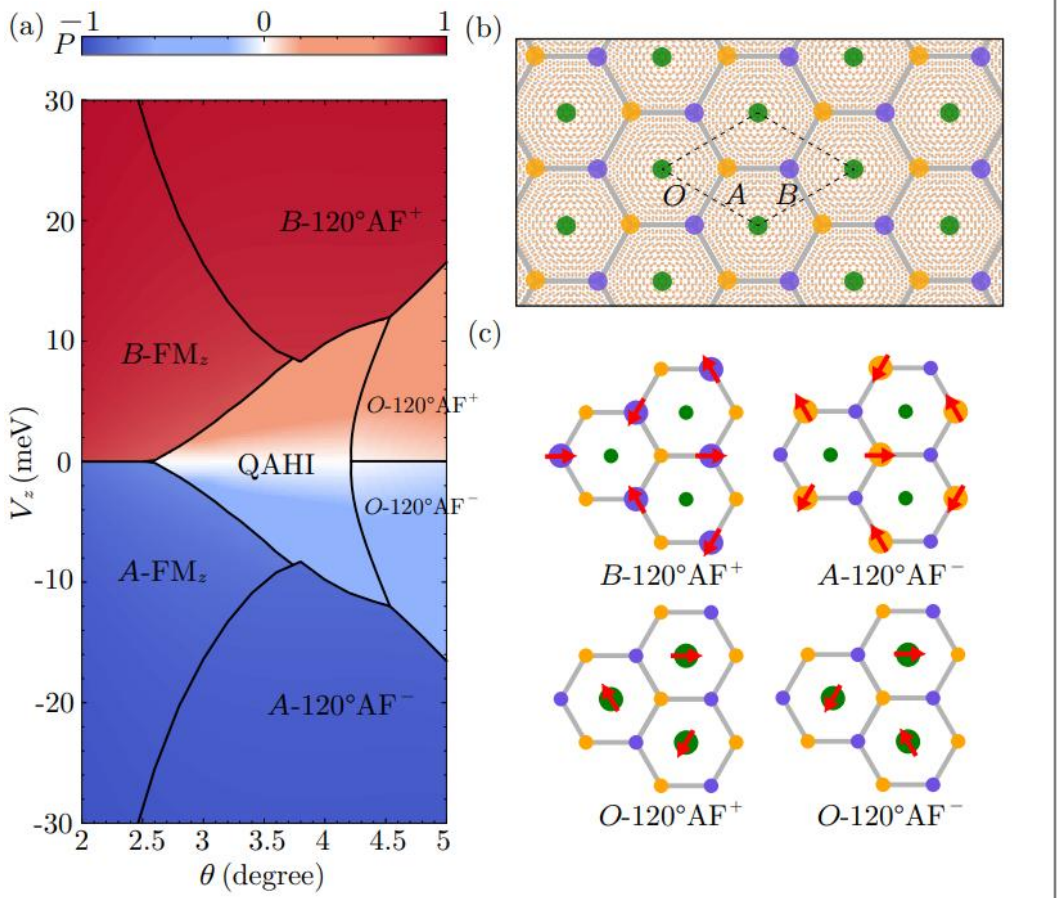

PRX **13**, 041026 (2023)
PRB **109**, L041106 (2024)

Experimental Phase Diagram

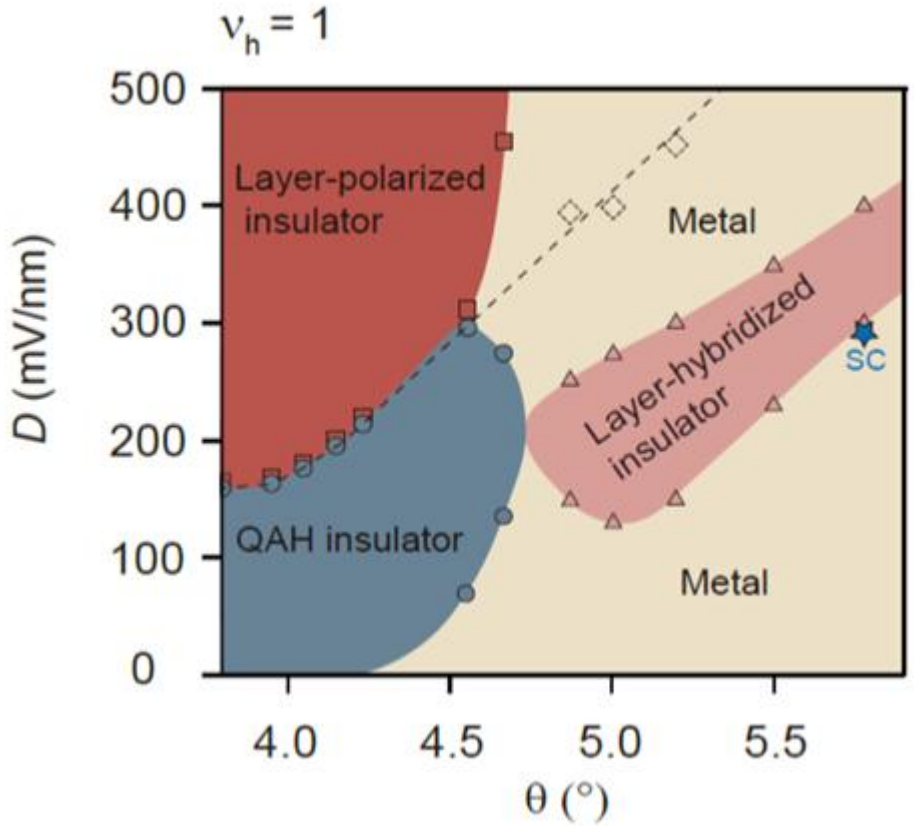

Z. Sun, …, T. Li, arXiv:2603.16412